Molecular Therapy
Nucleic Acids
Original Article

# Topical application of a CCL22-binding aptamer suppresses contact allergy

Anna Jonczyk,[1,6] Marlene Gottschalk,[2,6] Matthew S.J. Mangan,[3] Yasmin Majlesain,[2] Manja W. Thiem,[2,4] Lea-Corinna Burbaum,[2] Heike Weighardt,[2] Eicke Latz,[3] Günter Mayer,[5,7] and Irmgard Förster[2,7]

[1]Chemical Biology and Chemical Genetics, Life and Medical Sciences (LIMES) Institute, University of Bonn, 53121 Bonn, Germany; [2]Immunology and Environment, Life and Medical Sciences (LIMES) Institute, University of Bonn, 53115 Bonn, Germany; [3]Institute of Innate Immunity, University Hospital Bonn, 53127 Bonn, Germany; [4]Department of Microbiology and Immunology, The Peter Doherty Institute for Infection and Immunity, University of Melbourne, Melbourne, VIC 3000, Australia; [5]Centre of Aptamer Research and Development, University of Bonn, 53121 Bonn, Germany

**Allergic contact dermatitis is a prevalent occupational disease with limited therapeutic options. The chemokine CCL22, a ligand of the chemokine receptor CCR4, directs the migration of immune cells. Here, it is shown that genetic deficiency of CCL22 effectively ameliorated allergic reactions in contact hypersensitivity (CHS), a commonly used mouse model of allergic contact dermatitis. For the pharmacological inhibition of CCL22, DNA aptamers specific for murine CCL22 were generated by the systematic evolution of ligands by exponential enrichment (SELEX). Nine CCL22-binding aptamers were initially selected and functionally tested *in vitro*. The 29-nt DNA aptamer AJ102.29m profoundly inhibited CCL22-dependent T cell migration and did not elicit undesired Toll-like receptor-dependent immune activation. AJ102.29m efficiently ameliorated CHS *in vivo* after systemic application. Moreover, CHS-associated allergic symptoms were also reduced following topical application of the aptamer on the skin. Microscopic analysis of skin treated with AJ102.29m *ex vivo* demonstrated that the aptamer could penetrate into the epidermis and dermis. The finding that epicutaneous application of the aptamer AJ102.29m in a cream was as effective in suppressing the allergic reaction as intraperitoneal injection paves the way for therapeutic use of aptamers beyond the current routes of systemic administration.**

## INTRODUCTION

Allergic diseases, including allergic reactions of the skin, represent a significant global health concern, with a rising prevalence worldwide.[1] Manifesting as rash, itch, redness, and pain, these allergic reactions impose a substantial burden on individuals' quality of life.[1–3] Approximately 20% of the population suffers from contact allergies, such as allergic contact dermatitis (ACD), that can develop upon repeated exposure to allergens. ACD is a delayed hypersensitivity reaction initiated by highly reactive low-molecular-weight chemicals called haptens. During sensitization, haptens form a complex with endogenous proteins as carrier molecules, thereby forming an immunogenic neo-antigen that induces antigen-specific T cells, which upon a second contact with the hapten create a strong immune response leading to an allergic reaction.[4–6]

Central to the immunopathogenesis of allergic reactions is chemokine-mediated cell migration, orchestrating the recruitment of immune cells to sites of inflammation.[7,8] Among the chemokines implicated in allergic skin diseases, CCL17 and CCL22 stand out as critical mediators, binding to the chemokine receptor CCR4.[9–18] Elevated serum levels of CCL17 and CCL22 have been consistently observed in patients with atopic dermatitis, serving as potential biomarkers for disease severity and early diagnosis of ACD, particularly in children.[19–23]

In mice, both chemokines are constitutively detectable in the skin with an enhanced expression upon inflammation.[15] Furthermore, it was proven that CCR4-expressing T cells are recruited into the skin after the induction of ACD.[24] In contact hypersensitivity (CHS), the mouse model for ACD, a reduction of allergic symptoms was observed for CCL17-deficient ($CCL17^{-/-}$) mice,[17,18] whereas a deterioration of skin inflammation in CHS was detected in CCR4 knockout ($CCR4^{-/-}$) mice.[25] Remarkably, simultaneous antibody-mediated blockade of CCL17 and CCL22 did not inhibit CHS or attract activated T cells to the skin.[24,26] These unexpected findings might be explained by differential signal transduction of CCL17 and CCL22 following binding to CCR4, with a dominance of CCL22 over CCL17, a phenomenon called biased agonism.[27–29] Understanding the role of CCL22 in allergic diseases not only sheds light on the underlying mechanisms of allergic inflammation but it also underscores the importance of targeting chemokine signaling pathways for therapeutic interventions.

Received 17 April 2024; accepted 13 June 2024;
https://doi.org/10.1016/j.omtn.2024.102254.

[6]These authors contributed equally

[7]These authors contributed equally

**Correspondence:** Günter Mayer, Centre of Aptamer Research and Development, University of Bonn, Gerhard-Domagk-Straße 1, 53121 Bonn, Germany.
**E-mail:** gmayer@uni-bonn.de
**Correspondence:** Irmgard Förster, Immunology and Environment, Life and Medical Sciences (LIMES) Institute, University of Bonn, Carl-Troll-Straße 31, 53115 Bonn, Germany.
**E-mail:** irmgard.foerster@uni-bonn.de

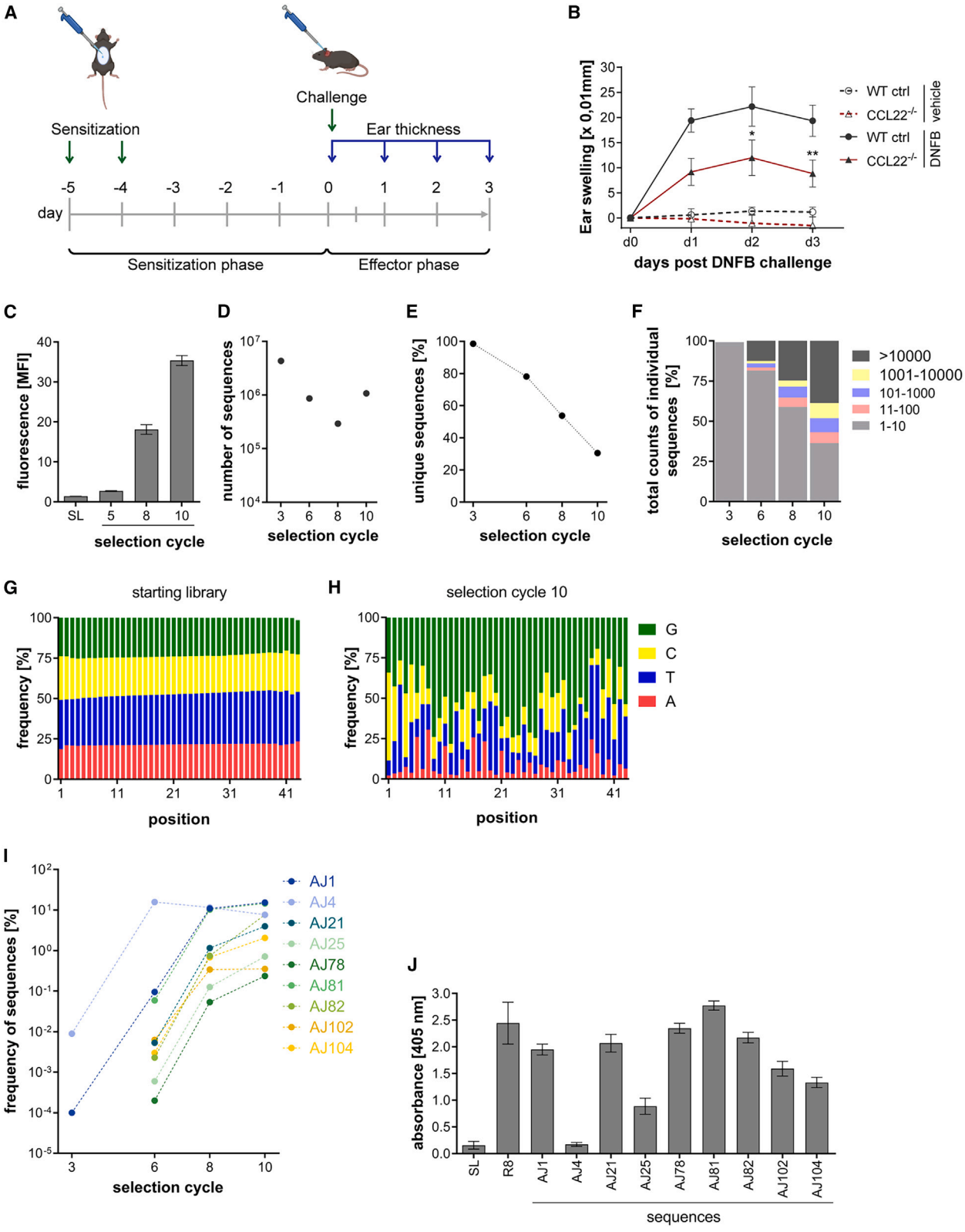


*(legend on next page)*

In a previous study, we demonstrated that blockade of CCL17 with RNA aptamers via a systemic application route successfully suppressed the allergic reaction in CHS.[18] As CCL22 has previously been described to preferentially attract regulatory T cells,[28,30] blockade of CCL22 could influence the development of allergic symptoms in CHS differently compared to CCL17. In the present study, we specifically assessed the role of CCL22 in CHS and evaluated the potential of a pharmacological blockade of CCL22 with DNA aptamers.

## RESULTS

### CCL22 deficiency ameliorates CHS

We first investigated the impact of a genetic deficiency of CCL22 on CHS. Mice were sensitized on 2 consecutive days with 0.25% 1-fluoro-2,4-dinitrobenzene (DNFB) in an olive oil-acetone mixture on the shaved abdomen to induce an immune response against the DNFB-self-peptide complex.[31] Four days later, mice were challenged with the same hapten or vehicle control on the ears to elicit allergic symptoms (Figure 1A). The change in ear thickness served as an indicator of the severity of the allergic reaction. Interestingly, CCL22-deficient ($CCL22^{-/-}$) mice[32] showed a significantly reduced ear swelling response in CHS compared with wild-type (WT) mice (Figure 1B). Thus, the CHS response of $CCL22^{-/-}$ mice was similar to that of $CCL17^{-/-}$ mice but different from $CCR4^{-/-}$ mice,[18,25] identifying CCL22 as an additional potential therapeutic target for the treatment of CHS.

### Selection of CCL22-specific DNA aptamers

To inhibit CCL22-dependent T cell migration pharmacologically, we developed CCL22-binding DNA aptamers by systematic evolution of ligands by exponential enrichment (SELEX).[33,34] We conducted 10 selection cycles, progressively increasing the stringency of selection (Figure S1; Table S1). To assess binding of the single-stranded (ss) DNA library to CCL22, we employed a flow cytometry-based interaction assay with Cy5-labeled ssDNA and CCL22 on magnetic beads. The DNA library obtained after 10 selection cycles showed over 25-fold higher binding compared to the starting library (SL) (Figure 1C). Enrichment of CCL22-binding ssDNA was observed after the 5th selection cycle, with DNA from the 8th cycle exhibiting a substantial 13-fold increase in binding compared to the SL. The DNA libraries obtained after selection cycles 3, 6, 8, and 10, as well as the SL were subjected to next-generation sequencing (NGS), with $10^5$–$10^6$ sequences analyzed per DNA library (Figure 1D). The analysis revealed a continuous decline in the number of unique sequences, reaching 30% after selection cycle 10 (Figure 1E). Likewise, the percentage of sequences with copy numbers exceeding 10,000 rose to 38% in selection cycle 10 (Figure 1F), suggesting a successful enrichment of DNA sequences. The distribution of nucleotides in the randomized region of the sequences also underwent changes from an equal distribution of the four nucleotides in the SL to guanine being the most frequently enriched nucleotide at many positions of the random region after 10 selection cycles (Figures 1G, 1H, and S2).

Based on the analysis of the libraries enriched during selection, nine of the most abundant sequences were chosen for further analysis (Figure 1I). Among these sequences, AJ1 (15.3%) and AJ81 (14.5%) emerged as the most enriched sequences in selection cycle 10. Throughout the selection cycles, stringency was gradually increased by reducing the amount of CCL22, increasing washing steps, and elevating the concentration of heparin as competitor. Consequently, sequences experiencing a decline in frequency after selection cycle 8, with the exception of the highly enriched sequence AJ4, were excluded from analysis due to their potential as being less specific binders.

To assess the binding capabilities of the nine selected sequences to CCL22, we used an enzyme-linked oligonucleotide assay (ELONA) (Figure 1J). Eight out of nine sequences displayed binding affinity toward CCL22. Notably, AJ4 did not recognize CCL22, suggesting it may have represented a non-specific, easily amplifiable sequence that accumulated during selection and subsequently diminished in frequency with higher competitor concentrations beyond selection cycle 8.

To test whether the aptamers functionally suppressed migration toward CCL22, we tested their inhibitory capacity using an *in vitro* transwell assay. This assay quantifies the migratory capacity of CCR4-expressing T cell lymphoma cells (BW5.1473 cells) toward CCL22 (12.8 nmol/well).[35] Aptamers were added in a 1:10-M ratio, an equimolar ratio, and a 10:1-M ratio to CCL22. Medium was used as a negative control and scrambled versions of the aptamers were tested in equimolar ratios. All tested aptamer candidates showed significant concentration-dependent inhibition of migration toward CCL22 (Figures 2A–2H).

Sequence analysis of the eight inhibitory aptamer candidates revealed three conserved sequence motifs (Figures 2I and 2J). Motif 1 was

**Figure 1. Identification of CCL22 as a target for treatment of contact allergy and development of aptamers targeting murine CCL22**

(A) Time line of the CHS mouse model. (B) The ear swelling response in $CCL22^{-/-}$ mice in the CHS model is significantly reduced compared to WT mice ($n = 7$, mean ± SEM). Data were tested for statistical significance by 2-way ANOVA with Bonferroni post hoc test (*$p$ = 0.01–0.05; **$p$ = 0.001–0.01; ***$p < 0.001$; ****$p < 0.0001$). (C) Flow cytometry-based interaction analysis of enriched DNA libraries from the SL and selection cycles 5, 8, and 10 to murine CCL22. (D) Frequency of unique sequences in selection cycles 3, 6, 8, and 10. The frequency was calculated by dividing the overall number of sequences by the number of unique sequences. (E) Number of sequence reads in the NGS analysis per selection cycle. (F) Fraction of sequences in the DNA population from selection cycles 3, 6, 8, and 10 sharing the indicated copy numbers. (G and H) Nucleotide distribution in the random region of the SL and library from selection cycle 10. The nucleotides are evenly distributed in the SL, and preferences for particular nucleotides at certain positions evolve during the selection. (I) Frequency of the most enriched sequences in selection cycles 3, 6, 8, and 10. Missing data points indicate that the sequence could not be detected in the NGS data of the respective round. (J) DNA sequences identified by NGS were analyzed for binding to murine CCL22 by ELONA ($n = 2$, mean ± SD).

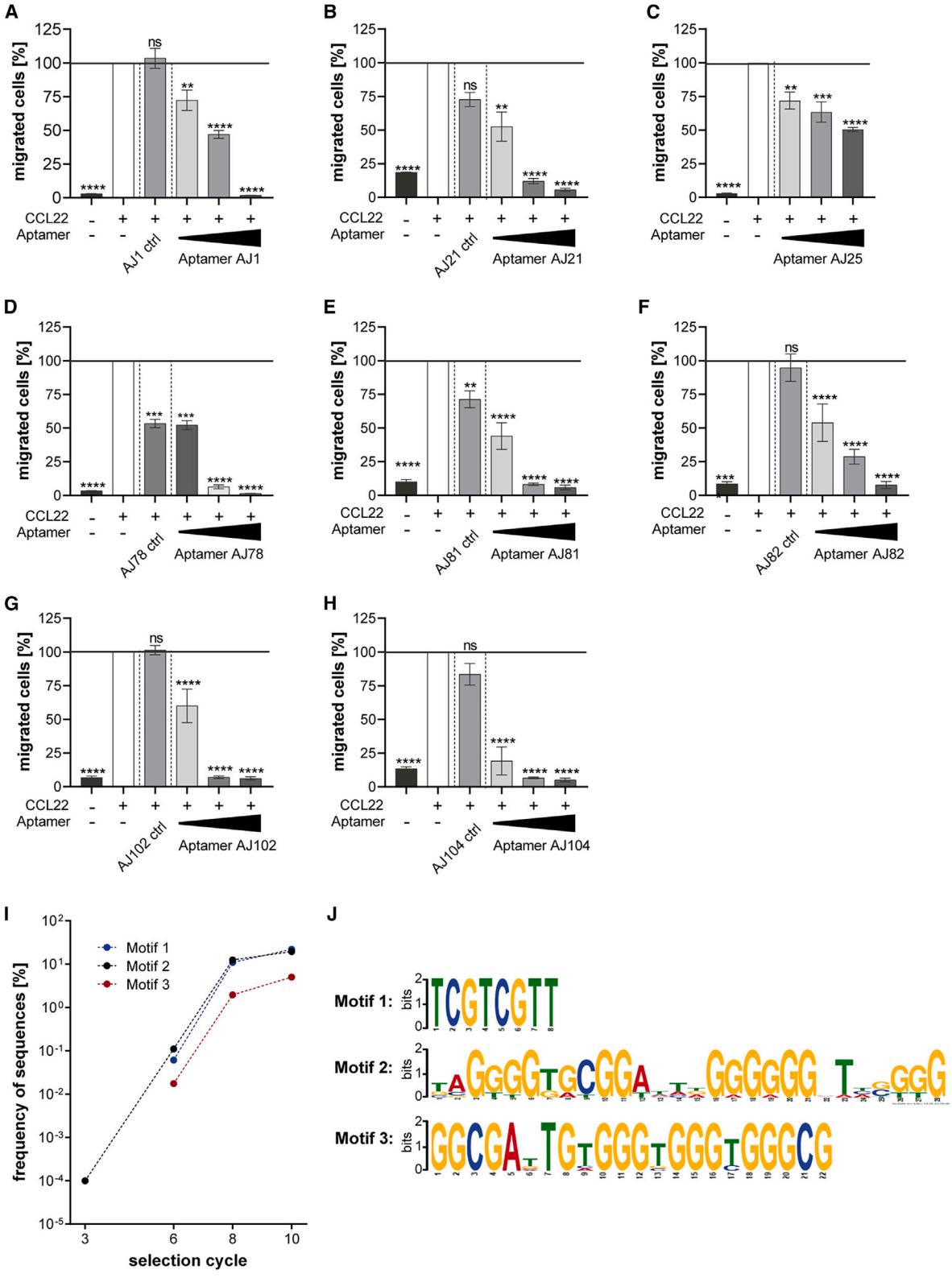


*(legend on next page)*

present in AJ81 and AJ82; motif 2 was found in AJ1, AJ25 and AJ104; and motif 3 was observed in AJ21 and AJ102. We selected AJ82 and AJ102 for further experiments as both aptamer candidates effectively inhibited CCL22-dependent migration in the transwell migration assay. Kinetic properties of the aptamer-protein interaction were assessed by flow cytometry and surface plasmon resonance (SPR) experiments. Flow cytometry (fluorescence-activated cell sorting) analysis revealed high affinity in the nanomolar range for both aptamers to CCL22 on magnetic beads: 146.1 nM for AJ82 and 146.7 nM for AJ102 (Figure S3). This high binding affinity was confirmed by SPR analysis using aptamer-coated sensor chips and concentration series of 1–270 nM unmodified CCL22 (Figures 3A and 3B). Equilibrium dissociation constants of 24.8 and 10.7 nM were found for AJ82 and AJ102, respectively. As depicted in Figures 3A–3C, a very slow dissociation of bound CCL22 from the aptamer-coated surface in running buffer was detected.

To assess the specificity of AJ82 and AJ102, interaction analysis via ELONA was conducted (Figure 3D). Results indicated that both aptamer candidates exhibited no cross-reactivity with human CCL22 and murine or human CCL17.

To remove unnecessary nucleotides in the aptamer candidates, while keeping nucleotides essential for target binding, we truncated AJ82 and AJ102 based on structure predictions by Mfold.[36] For AJ82, a structure featuring two hairpins was predicted. Consequently, we explored the necessity of the individual hairpin structures (82.27 and 82.19) for binding, which, when isolated, did not bind CCL22 (Figures 4A and 4B). Furthermore, a truncated version of AJ82.59 was generated by removing nucleotides from the 3′ and 5′ ends close to the hairpin regions. To stabilize the stem region of the hairpin at the 3′ end, a point mutation from dA to dC was inserted at position 49, resulting in increasing binding intensity. Further truncations resulted in sequence 82.51. The removal of additional nucleotides from the 3′ or 5′ ends resulted in decreased or negligible binding to CCL22 (Figure 4A). Likewise, sequence AJ102 was truncated based on the Mfold structure bearing three hairpins (Figure 4C). Nucleotides were systematically removed, leading to the shortest binding sequence AJ102.29 (Figure 4D). Truncation of additional nucleotides from the 5′ (AJ102.24) or 3′ end (AJ102.25) resulted in reduced or negligible binding to CCL22. Point mutations in the region of the enriched motif within AJ102.29 revealed that mainly dG positions were essential for target binding (Figure 4E). To identify potential G-quadruplex (GQ)-forming sequences within AJ102.29, we used the prediction tool QGRS Mapper.[37] QGRS Mapper proposed two G-tetrad layers from guanine residue 21 to 39, with a G-score of 16. However, experimental analysis via circular dichroism (CD) of AJ102 did not confirm the formation of a GQ structure (Figure S4). Similarly, no GQ structure was validated for aptamer AJ82, despite its GC content of 60.5% and the G-score of 21 indicating the likelihood of a G-tetrad layers spanning from guanine 37 to 62.

Following truncation, the binding properties of both aptamers were analyzed to ensure that truncation did not cause loss of affinity or specificity. Notably, both aptamers showed improved affinities of 29.3 nM for AJ82.51 and 63.6 nM for AJ102.29 to CCL22, as determined by flow cytometry (Figures 3C and S3). Furthermore, the specificity of AJ82.51 and AJ102.29 was assessed against a variety of related and unrelated chemokines, demonstrating that specificity was maintained after truncation (Figures 4F and 4G). A 20-kDa 5′-polyethylene glycol tail and a 3′-dT cap structure (AJ82.51m, AJ102.29m) were added to increase the half-life and prolong resistance to renal clearance.[38–40] Whether the modifications influenced the ability of the aptamers to inhibit CCL22-dependent migration was tested by performing transwell assays (Figure 5A). The inhibitory capacity of the modified truncated aptamers AJ82.51m (Figure 5B) and AJ102.29m (Figure 5C) were comparable to their parental aptamers. Thus, the modifications did not alter functionality.

### Inhibitory potential of CCL22-specific aptamers *in vivo*

Prior to *in vivo* application, both aptamers were tested for activation of DNA sensing pattern recognition receptors, which could lead to adverse immune responses (Figure 6). We determined the propensity of the aptamers to trigger Toll-like receptor activation by assessing the secretion of tumor necrosis factor (TNF) in immortalized murine embryonic stem cell-derived immortalized macrophages. This revealed that AJ82.51 and AJ82.51m, and to a lesser extent, their scrambled controls, induced TNF secretion (Figure 6A). Thus, the application of AJ82.51m might lead to the induction of innate immune responses *in vivo*, and therefore it is not suitable for potential use in the CHS mouse model. In contrast, AJ102.29m did not induce TNF secretion (Figure 6B). To optimize the application time points of AJ102.29m during CHS, the stability of the aptamer in mouse serum and in DPBS was analyzed in comparison to the unmodified version AJ102.29 (Figure S5). Both unmodified AJ102.29 (Figures S5A and S5C) and modified AJ102.29m (Figures S5B and S5D) were stable in DPBS during the first 48 h. In mouse serum, hydrolysis was observed, which led to a decrease to 26% (AJ102.29) and 11% (AJ102.29m) of the original amount of aptamer within the first 2 h. After 48 h, 10% (AJ102.29) and 2% (AJ102.29m) of the DNA was still intact. Incubation with DNAse I resulted in the same value as for the no-template controls (Figure S5E). Therefore, to ensure sufficiently

**Figure 2. Aptamer-dependent inhibition of migration toward mCCL22 *in vitro* and motifs enriched during CCL22 SELEX**

(A–H) Migration of BW5147.3 cells toward CCL22 (12.8 nM) was measured in a transwell migration assay in the presence of aptamers. Full-length aptamers AJ1 (A), AJ21 (B), AJ25 (C), AJ78 (D), AJ81 (E), AJ82 (F), AJ102 (G), and AJ104 (H) were tested in a 1:10 M ratio (1.28 nM), an equimolar ratio (12.8 nM), and a 10:1 M ratio (128 nM) along with their scrambled control sequences. As control, migration without the addition of CCL22 or aptamers, as well as the migration toward CCL22 only were measured. Statistical significance was calculated against migration toward CCL22 and tested by using ordinary 1-way ANOVA with post hoc Bonferroni test with $n = 3–16$ (mean ± SEM, $^{*}p = 0.01–0.05$; $^{**}p = 0.001–0.01$; $^{***}p < 0.001$; $^{****}p < 0.0001$). (I) Frequency of 3 motifs common among the most enriched sequences. Motif 1 is found in AJ81 and AJ82. Motif 2 is found in AJ1, AJ25, and AJ104. Motif 3 is found in AJ21 and AJ102. (J) Sequences of the motifs identified by MEME Suite.

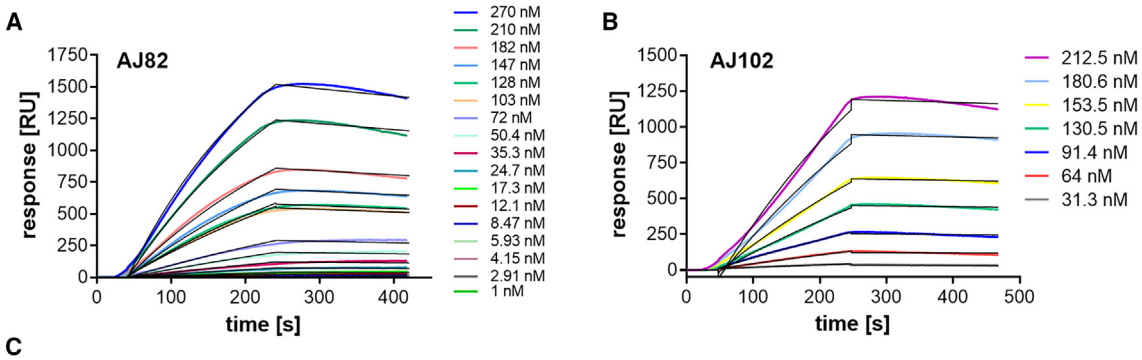


C

| | FACS | SPR | | |
|---|---|---|---|---|
| sequence | mCCL22 $K_D$ [nM] | mCCL22 $K_D$ [nM] | $k_a$ [$10^4$ $M^{-1}$ $s^{-1}$] | $k_d$ [$10^{-4}$ $s^{-1}$] |
| **AJ82** | **146.1 ± 20.3** | **24.80 ± 1.00** | **3.87 ± 0.09** | **1.58 ± 0.11** |
| **AJ82.51** | **29.3 ± 3.0** | **nd** | **nd** | **nd** |
| **AJ102** | **146.7 ± 11.2** | **10.70 ± 1.87** | **1.31 ± 0.01** | **1.41 ± 0.30** |
| **AJ102.29** | **63.6 ± 4.0** | **nd** | **nd** | **nd** |

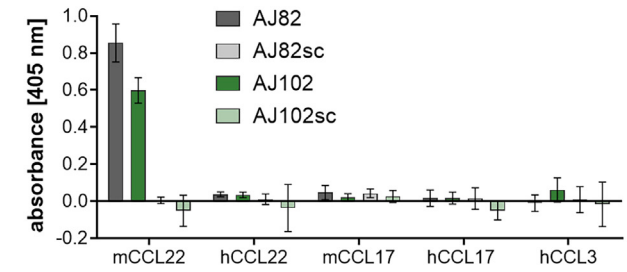


**Figure 3. Binding affinity and specificity of aptamer AJ82 and AJ102**

(A and B) Concentration-dependent binding of aptamer AJ82 (A) and AJ102 (B) measured by SPR using murine CCL22 as analyte and biotinylated aptamers as immobilized ligands ($n$ = 2, mean ± SD). (C) Table of kinetic properties of the aptamers AJ82, AJ82.51, AJ102, and AJ102.29 as measured by flow cytometry or SPR. nd, not determined. (D) Interaction analysis of aptamer AJ82 and AJ102 with murine CCL22, human CCL22, murine CCL17, human CCL17, and human CCL3 measured by an ELONA ($n$ = 2–3, mean ± SD).

high levels of AJ102.29m in the circulation, two consecutive intraperitoneal injections of 10 nmol AJ102.29m, 12 h apart, were used to investigate the therapeutic potential of AJ102.29 *in vivo*. As a suitable application time point, we chose to apply the aptamer during the challenge phase—in other words, directly after the challenge and 12 h post challenge (Figure 7A). Using this application regimen, AJ102.29m significantly reduced ear swelling in WT mice, whereas the scrambled control did not affect ear swelling (Figure 7B). CCL22$^{-/-}$ mice showed the greatest decrease in ear swelling. Thus, pharmacological blockage of CCL22 by intraperitoneally injected AJ102.29m significantly reduced ear swelling after DNFB challenge.

For the potential treatment of ACD, topical application to the affected skin would be advantageous compared to intraperitoneal or intravenous administration, because it is non-invasive and can be applied only to the affected sites, posing less risk of unwanted systemic side effects. Therefore, we first performed an *ex vivo* skin test to evaluate whether the aptamer AJ102.29 could penetrate the skin. In this experiment, we used fluorescently labeled AJ102.29 in an amphiphilic DAC cream, a basic preparation according to the German Drug Codex, which is commonly used by dermatologists and pharmacologists for the topical application of drugs.[41] Using Franz cell diffusion chambers, we confirmed the penetration of AJ102.29 into the epidermis and dermis of murine ear skin (Figures 7C and 7D). The penetration was not dependent on the ability of AJ102.29 to bind CCL22, as we also observed penetration of AJ102.29ctrl into the epidermis and dermis similarly to AJ102.29 (Figures S6A and S6B), but detected no signal when applying DAC cream only (Figure S6C). In addition, we tested the ability of the non-supplemented DAC cream to ameliorate CHS, because beneficial effects of emollients on contact allergy have been described.[42] However, we did not observe a difference between WT mice treated

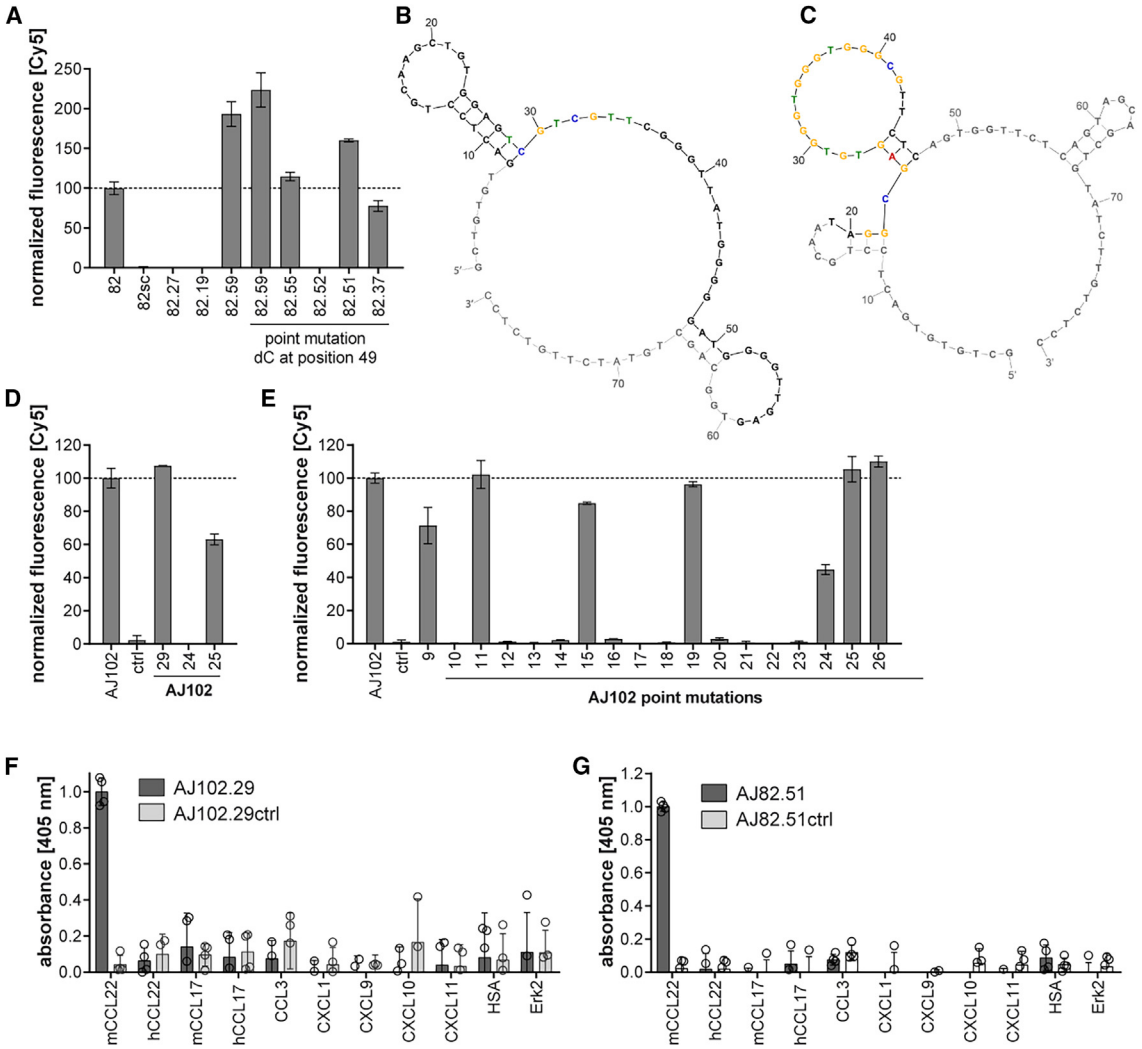


**Figure 4. Truncation of aptamers and specificity of AJ82.51 and AJ102.29**

(A) Flow cytometry-based interaction assay of truncated variants of aptamer AJ82 with CCL22. AJ82 was truncated from 80 to 51 nt, including an initial point mutation at position 49 (dA to dC) for stabilization of the stem structure. (B and C) Structure predictions of aptamer AJ82 (B) and AJ102 (C) as predicted by Mfold web server. Shown is the prediction for the full-length sequence. Colored nucleotides indicate the motif 1 in AJ82 and motif 2 in AJ102. Gray nucleotides were truncated. (D) Flow cytometry-based interaction assay of truncated variants of aptamer AJ102 with CCL22. AJ102.29 was truncated from 80 to 29 nucleotides. AJ102.24 was truncated from the 5′ end, while AJ102.25 was truncated from the 3′ end ($n$ = 2, mean ± SD). (E) Flow cytometry-based interaction analysis with AJ102 and point mutants within the motif region ($n$ = 2, mean ± SD). Mainly dG positions are involved in target binding. (F and G) Interaction analysis of truncated 500-nM aptamers AJ82.51 (F) or AJ102.29 (G) with related chemokines human CCL22, murine and human CCL17, human CCL3, human CXCL1, human CXCL9, human CXCL10, human CXCL11 and unrelated proteins human serum albumin (HSA) and mitogen-activated protein kinase 1 (Erk2) measured by ELONA ($n$ = 2, mean ± SD).

with or without DAC cream and could only detect a reduction of allergic symptoms in control mice deficient for CCL17 (Figure S7). To investigate the potential of topically applied AJ102.29m to suppress allergic symptoms in CHS, 10 nmol AJ102.29m or its scrambled control in DAC cream was administered at the same time points as before. Notably, mice that received AJ102.29m showed a significant decrease in ear swelling at the DNFB-treated ears compared with mice treated topically with the scrambled control aptamer (Figure 7E). Compared with systemic application (Figure 7B), the inhibition of the allergic symptoms appeared slightly more effective, close to that observed in CCL22$^{-/-}$ mice. Thus, AJ102.29m retained a similar inhibitory potential when administered topically in DAC cream compared to systemic application and was able to effectively suppress CHS via both routes.

## DISCUSSION

In this study, we demonstrate both the importance of CCL22 for development of CHS, as well as successful suppression of allergic symptoms through pharmacological inhibition of CCL22 with DNA aptamers. These findings are consistent with our previous study

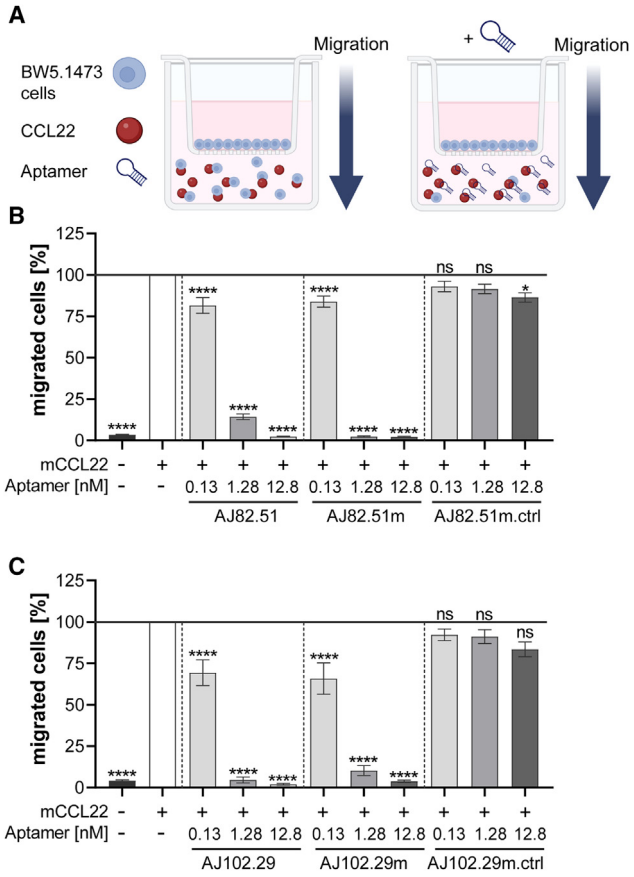


**Figure 5. Inhibition of CCL22 mediated cell migration *in vitro* by truncated and modified aptamers AJ82.51 and AJ102.29**

(A) Schematic representation of the transwell migration assay. BW5147.3 cells were placed in the upper layer of the insert with a permeable membrane, and CCL22 was added at different concentrations to the lower compartment. Following an incubation period, the cells that migrated through the membrane were quantified by flow cytometry. (B and C) Migration of BW5147.3 cells toward CCL22 (12.8 nM) was measured in a transwell migration assay in the presence of aptamers. Truncated aptamers AJ82.51 (B) and AJ102.29 (C) and truncated and modified aptamers AJ82.51m (B) and AJ102.29m (C) were tested in a 1:10 M ratio (1.28 nM), an equimolar ratio (12.8 nM), and a 10:1 M ratio (128 nM). As control, migration toward the control sequences AJ82.51 ctrl, AJ102.29 ctrl and AJ82.51m ctrl, AJ102.29m ctrl (12.8 nM), without the addition of CCL22 or aptamers, as well as the migration toward CCL22 only were measured. Statistical significance was calculated against migration toward CCL22 and tested by using ordinary 1-way ANOVA with post hoc Bonferroni test, with $n$ = 7–15 (mean ± SEM; ****$p < 0.0001$). ns, not significant.

in which we demonstrated that CCL17, another ligand of CCR4, was required for ear swelling and immune cell infiltration in CHS, and that the pharmacological blockade of CCL17 by RNA aptamers could reverse this.[18] Despite the known biased agonism of CCL17 and CCL22 regarding signal transduction through CCR4,[27,43,44] we observed that genetic deficiency of either chemokine led to a similar amelioration of CHS, whereas genetic absence or pharmacological blockade of CCR4 enhances the allergic reaction or even induces autoimmunity.[25,45–49] Thus, biased agonism of CCL17 and CCL22 apparently does not explain the different outcome of either CCL17 or CCL22 blockade and that of CCR4 deficiency or blockade. Alternatively, our findings may be explained by a scenario that (1) CCL17 and CCL22 are essential for immune cell infiltration during different phases of extravasation into or migration within the skin[50,51] or (2) CCR4 plays a redundant role with other chemokine receptors in the attraction of effector T cells to the skin, whereas it appears to be essential for the recruitment of regulatory T cells to sites of inflammation or homing into the tumor microenvironment.[16,52,53] It should also be noted that our data are not in line with earlier reports that antibody-mediated inhibition of both CCL17 and CCL22 did not result in the amelioration of CHS.[24,26] In these studies, additional blockade of the CCR10 ligand CCL27 was required to inhibit the CHS response. A possible explanation for this discrepancy could be a higher affinity of the inhibitory aptamers to their targets, or a better accessibility of the targets by aptamers as compared to antibodies within the skin. In any case, the inhibitory efficiency of selective blockade of either CCL17 or CCL22 is in agreement with the relative resistance of CCL17- or CCL22-deficient mice to CHS. Consistently, CCL22 levels are elevated in the serum of patients with ACD, supporting its potential as a target for the development of therapeutics for contact allergy.[19] As administration of the CCR4 antibody mogamulizumab leads to severe adverse skin disorders when used as a treatment for T cell lymphoma, Sézary syndrome, or mycosis fungoides,[45–49] blocking CCL22 by DNA aptamers might also be of relevance as an alternative or supplemental option in combination with mogamulizumab in cancer therapy.[45]

Aptamers combine the advantageous properties of small molecules and antibodies in that they are small, specific, generated by chemical synthesis, and less likely to elicit an adverse immune response.[54–56] To date, effective topical application of nucleic acids has been reported mainly in combination with nanoparticles, liposomes, peptides, or using lasers.[57] Although topical application of RNA aptamers has been reported,[58,59] the doses applied were up to 57 times higher than the one used in our study and required application of the aptamer before induction of a skin lesion. A relevant feature of the aptamer AJ102.29m used in this study is its short length of only 29 nt, which may facilitate penetration of the aptamer through the epidermis following topical application. To the best of our knowledge, our study is the first to demonstrate effective topical delivery of a DNA aptamer in a cream using the same dose that resulted in efficient systemic inhibition of the targets. We also performed comprehensive control experiments and show direct evidence of penetration of both AJ102.29m and its scrambled control aptamer into the epidermis and dermis, whereas only AJ102.29m was able to functionally block allergic skin inflammation.

In summary, we demonstrate that the chemokine CCL22 promotes the development of CHS and that CCL22-specific DNA aptamers significantly reduce allergic symptoms associated with CHS in mice. Furthermore, we demonstrate that the DNA aptamers have therapeutic benefit when they are applied directly to the skin in a cream formulation, which extends their application beyond the current routes of

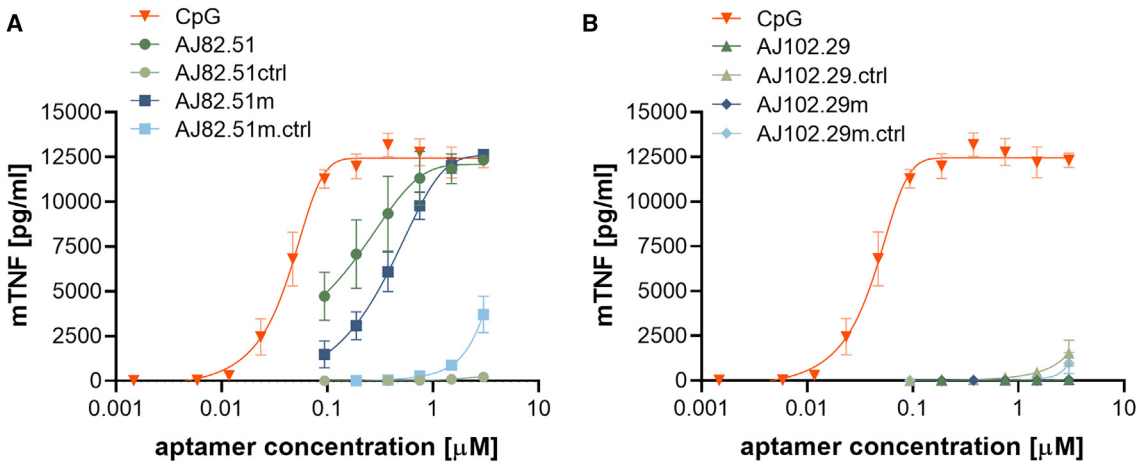


**Figure 6. AJ82.51 but not AJ102.29 induce TNF secretion in macrophages**

(A and B) Immortalized murine embryonic stem cell-derived macrophages were incubated with increasing concentrations of the immunostimulatory TLR9 ligand CpG along with modified and unmodified aptamers AJ82.51 (A) or AJ102.29 (B) together with their respective control sequence. After 24 h of incubation, the TNF secretion in the supernatant was measured.

administration of aptamers. For topical application, in particular, the shorter *in vivo* half-life of aptamers as compared to antibodies may also be beneficial. In this case, repeated application on the affected skin is not problematic, and the treatment can be readily terminated if required, depending on the actual need. Furthermore, the results of this study have far-reaching implications, as they imply that topical application of aptamers in creams may be effective not only in the treatment of skin allergies but also in other skin-related diseases, such as melanoma.

## MATERIALS AND METHODS

### Selection of CCL22-binding aptamers

The DNA library was purchased from Ella Biotech and is composed of a 43-nt randomized region flanked by primer binding sites (GCTGTGTGACTCCTGCAA-N43-GCAGCTGTATCTTGTC TCC). Recombinant murine CCL22 (PeproTech) was immobilized on carboxyl beads (Thermo Scientific) (Table S1). In the first selection cycle, the SL (500 pmol) was incubated with unmodified carboxyl beads (30 μL) in a total volume of 300 μL selection buffer (20 mM HEPES, 110 mM NaCl, 5 mM KCl, 1 mM $MgCl_2$, pH 7.4). The sample was incubated for 30 min at 37°C and 1,000 rpm, and the supernatant was used for incubation with CCL22 carboxyl beads (30 μL, ∼833 pmol CCL22) for 30 min at 37°C and 1,000 rpm. The beads were washed twice with selection buffer, and bound ssDNA was eluted by heating the CCL22 beads in double-distilled (dd)$H_2O$ (50 μL) at 80°C for 5 min. The DNA was amplified using the forward primer 5′-GCTGTGTGACTCCTGCAA-3′ and reverse primer 5′-GGAGA-CAAGATACAGCTGC-3′. ssDNA was generated by lambda exonuclease (Thermo Fisher) digestion for 30 min at 37°C, and the ssDNA was purified over silica columns (PCR Clean-up, Macherey-Nagel). The amount of DNA obtained after purification was used for the next selection cycle. To gradually increase the selection pressure, the washing steps were increased while the amount of CCL22 was decreased, and heparin was added as competitor from the 6th selection cycle on (Table S1). All oligonucleotides used in this study are listed in Table S2.

### Coupling of CCL22 to magnetic beads

Different amounts of recombinant murine CCL22 (PeproTech) as stated in Table S1 were added to carboxyl beads (30 μL) in 25 mM MES buffer (pH 5) and incubated for 4 h at 4°C with 20 rpm tilt rotation. Beads were washed with Dulbecco's PBS (DPBS; Gibco) containing 1 mg $mL^{-1}$ BSA and 0.05% Tween 20. Unreacted carboxylic acid groups were blocked by incubation in 50 mM Tris (pH 7.4) for 15 min at 4°C. CCL22 beads were stored in DPBS with 0.01 mg $mL^{-1}$ BSA at 4°C for a maximum of 3 days. Coupling of CCL22 on carboxyl beads was validated by staining with an anti-CCL22 antibody (mouse α-murine CCL22 [R&D Systems]) and fluorescently labeled secondary antibody (goat α-mouse Alexa Fluor 647 (Jackson ImmunoResearch) by flow cytometry.

### ELONA

A total of 20 μL of a 1-μg $mL^{-1}$ protein solution in PBS was coated on hydrophobic plates (96-well microplate, half-well, Microlon 600, Greiner Bio One) overnight at 4°C while shaking slightly. Unbound protein was removed by washing 3 times with 100 μL DPBS (Gibco) containing 0.05% Tween 20. Wells were blocked with 5% BSA (100 μL) solution in DPBS for 2 h at room temperature while shaking slightly. Wells were washed 1 time with selection buffer (see description of the respective selection) and incubated for 30 min at 37°C and 50 rpm with biotinylated aptamer solution (500 nM, 20 μL) in selection buffer. Afterward, the wells were washed 2 times with selection buffer (100 μL) and incubated with a 1:1,000 dilution of streptavidin-biotin horseradish peroxidase complex (50 μL) (GE Healthcare) in selection buffer for 30 min at 37°C while shaking slightly. Wells were washed 2 times with

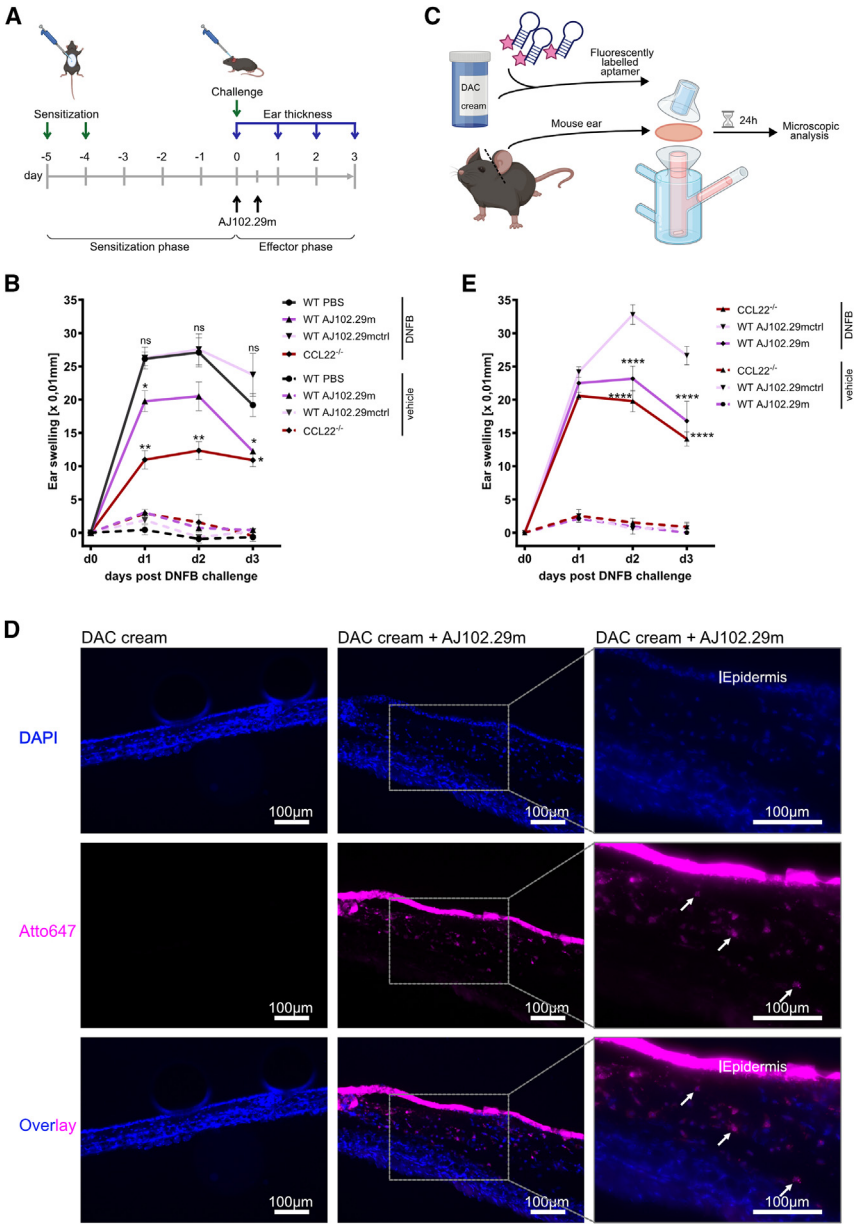


**Figure 7. *Ex vivo* and *in vivo* application of AJ102.29 results in effective reduction of contact hypersensitivity symptoms and penetration of the skin**

(A) Time line of the contact hypersensitivity model application time points of AJ102.29m. (B) Ear swelling of WT mice that received PBS, 10 nmol AJ102.29m, or 10 nmol AJ102.29mctrl intraperitoneally and of CCL22$^{-/-}$ mice 24 h (day 1), 48 h (day 2), and 72 h (day 3) after application of DNFB (solid lines) or vehicle (dashed lines). Data were tested for statistical significance by 2-way ANOVA with Bonferroni post hoc test ($n$ = 6 WT PBS, WT AJ102.29 ctrl, WT AJ102.29 ctrl, $n$ = 3 CCL22$^{-/-}$, mean ± SEM; *$p$ = 0.01–0.05; **$p$ = 0.001–0.01; ***$p$ < 0.001; ****$p$ < 0.0001). (C) Schematic representation of the Franz-diffusion cell assay. Fluorescently labeled aptamer in DAC cream was placed in the donor compartment. The skin of a mouse ear was placed horizontally between the donor and receptor compartment filled with RPMI medium. After 24 h the skin sample was stained with DAPI and analyzed by fluorescent micrsocopy to investigate skin penetration of the aptamer. (D) DAPI-stained sections of mouse ears treated with DAC cream with or without Atto647 labeled AJ102.29 (10 pmol mg$^{-1}$) in an *ex vivo* Franz-diffusion cell assay. (E) Ear swelling of WT mice that received PBS, 10 nmol AJ102.29m, or AJ102.29mctrl mixed in a DAC cream and topically applied on the ear at the time of and 12 h after challenge, and of CCL22$^{-/-}$ mice 24 h (day 1), 48 h (day 2), and 72 h (day 3) after application of DNFB (solid lines) or vehicle (dashed lines) ($n$ = 4–5, mean ± SEM). Data were tested for statistical significance by 2-way ANOVA with Bonferroni post hoc test ($n$ = 5 per group, mean ± SEM; *$p$ = 0.01–0.05; **$p$ = 0.001–0.01; ***$p$ < 0.001; ****$p$ < 0.0001).

selection buffer (100 µL) and incubated with ABTS substrate solution (50 µL) (Thermo Scientific) for 30 min at room temperature while shaking slightly. Absorbance at 405 nm was measured using a TECAN spectrophotometer (NanoQuant Infinite M200).

### Flow cytometry-based binding assay

For flow cytometry measurements, respective sequences were amplified using 5′-Cy5-labeled forward primers. Stated concentrations of Cy5-labeled ssDNA were incubated with protein-coupled beads (1 µL) in selection buffer in a final volume of 20 µL. Samples were incubated for 30 min at 37°C and 1,000 rpm. Beads were washed twice with selection buffer (200 µL) and finally resuspended in 100 µL, and the fluorescence intensity was measured by flow cytometry (FACSCanto II, BD Bioscience).

### SPR

SPR measurements were performed using a Reichert SR7000DC. Running buffer (20 mM HEPES, 110 mM NaCl, 5 mM KCl, 1 mM $MgCl_2$, pH 7.4) and regeneration buffer (100 mM EDTA, 50 mM NaCl, 0.01% SDS) were filtered (0.22 µm) prior to use. Biotinylated aptamer (50 nM in 0.5 M NaCl) was immobilized on a streptavidin-coated sensor chip (SCR SAD500L) at 25°C and a flow rate of 10 µL min$^{-1}$ according to the manufacturer's instructions. The control aptamer was immobilized as non-binding control with the same response unit on the reference cell. The protein was injected at 37°C with a flow rate of 35 µL min$^{-1}$ for 270 s with a dissociation phase of 200 s. The affinity was determined with TraceDrawer 1.9.2 using OneToOne model fit.

### NGS

To identify individual aptamer sequences, DNA libraries obtained from the 3rd, 6th, 8$^{th}$, and 10th selection cycle were analyzed by

NGS. The preparation of NGS samples was performed as described in Tolle and Mayer.[60] In brief, the samples were PCR amplified using primers containing different bar codes for each selection cycle. The DNA of all 12 samples was then mixed and prepared using the TruSeq DNA PCR-Free LT Kit (Illumina) according to the manufacturer's instructions. Libraries were clustered at 7 pM supplemented with PhiX on a TruSeq SR version 3 flow cell and sequenced over 75 bp on a HiSeq1500 (Illumina). The NGS data for the respective selections were analyzed using in-house developed software.

### Aptamer stability assay

A total of 100 pmol modified or unmodified AJ102.29 and AJ102.29ctrl were incubated either in DPBS or mouse serum (Biowest) at 37°C for 0, 2, 4, 6, 8, 24, 48, 72, 96, 120, 168, 216, or 288 h in a final volume of 100 µL. At each time point, 1 µL sample was taken and diluted 1:500. In addition, 1 µL aptamer (t = 0 h) was digested using DNase I (Roche) for 30 min at 37°C before performing qPCR. The samples were amplified by qPCR (Bio-Rad CFX96 Real-Time System) using the reverse primer 5′-GAGAACGCCCACCC-3′ and the forward primer 5′-TAGGC GAGTGTGGGT-3′ and the PowerSYBR Green PCR Master Mix (Applied Biosystems). Forty PCR cycles were performed along with a serial dilution of the t = 0 h samples as standards. The data were analyzed using the CFX Maestro software (Bio-Rad) and the resulting cycle threshold values are depicted as reciprocal values.

### CD spectroscopy

CD spectroscopy was performed to investigate whether AJ102 forms a GQ structure. The spectrum of the sequence h17_11 does not contain G-triplets and was thus recorded as negative control. The spectrum of sequence C10.36[61] folds into a parallel GQ and was recorded as positive control. For the measurement, a dilution of ssDNA (10 µM) was prepared either in $ddH_2O$ or in selection buffer (20 mM HEPES, 110 mM NaCl, 5 mM KCl, 1 mM $MgCl_2$, pH 7.4). Samples were heated to 85°C for 3 min, cooled to 37°C, and incubated for a further 30 min at 37°C. The samples were transferred into a cuvette directly before the measurement with the Jasco J-810 Spectropolarimeter. Spectra were recorded between 200 and 320 nm, and the data were evaluated with Prism 8.0.

### TNF homogeneous time-resolved fluorescence assay

Immortalized murine embryonic stem cell-derived macrophages were seeded in 96-well plates, at 80,000 cells per well in complete DMEM at a final volume of 90 µL. After an incubation period of 1 h, 10 µL of either the aptamer or the CpG oligonucleotide (employed as a control) were added such that the final concentration was a series ranging from 0.09 to 3 µM. Following the incubation period of 24 h at 37°C, 50 µL cell-free supernatant was collected from each well. The cell-free supernatants were assessed for TNF using homogeneous time-resolved fluorescence (Cisbio) according to the manufacturer's instructions as an indicator of immunogenicity.

### Transwell migration assay

The transwell migration assay was performed based on the assay described in Fülle et al.[18] and adapted to a 96-well system. BW5147.3 cells were thawed 1 day prior to the assay and cultured (RPMI + 10% fetal calf serum [FCS], penicillin-streptomycin, L-glutamine). On the day of the assay, cells were starved for 3.5 h in starvation medium (RPMI + 0.5% FCS, penicillin-streptomycin, L-glutamine) at 37°C 5% $CO_2$. The lower chambers of 96-well transwell plates (5 µm pores, Corning HTS Transwell 96-well permeable supports) were filled with starvation medium (235 µL) and supplemented with recombinant murine CCL22 (PeproTech) (12.8 nM) and aptamer or the matching aptamer control in a 1:10 M ratio (1.28 nM), an equimolar ratio (12.8 nM), and a 10:1M ratio (128 nM). The starved cells were adjusted to a concentration of $6.7 \times 10^5$ cells/mL and a 75-µL cell suspension was filled into the upper chambers. After a migration period of 2.5 h at 37°C 5% $CO_2$ the transmigrated cells in the lower chamber were harvested and quantified using flow cytometry (FACS Symphony, BD Biosciences).

### Mice

All mice were kept in the animal facility of the LIMES Institute, University of Bonn, under specific pathogen-free conditions. The experiments were performed with female 8- to 12-week-old WT mice (C57BL/6J-RCCHsd; Envigo), $CCL22^{-/-}$[32] mice or $CCL17^{-/-}$ mice.[17] All experiments were performed according to German and Institutional guidelines for animal experimentation and were approved by the government of North Rhine-Westphalia (Az. 81-02.04.2021.A092).

### CHS

Mice were sensitized with DNFB (Sigma-Aldrich) (70 µL, 0.25%) in acetone/olive oil (5:1) on the shaved abdomen at day −5 and day −4. At day 0 mice were anesthetized to measure the baseline ear thickness using a gauge caliper. Then, the animals were challenged with DNFB (10 µL, 0.3%) in acetone/olive oil on the dorsal and ventral side of the right ears. The left ears were treated with the vehicle only. The ear thickness was measured blinded 24 h (day 1), 48 h (day 2), and 72 h (day 3) after the application of DNFB, and the swelling was calculated by subtraction of the individual baseline thickness (day 0) at the end of the experiment. For the aptamer injections, AJ102.29m or AJ102.29mctrl (10 nmol) was administered intraperitoneally in PBS at the time of the challenge and 12 h post DNFB challenge. For the topical application AJ102.29m or AJ102.29mctrl (10 nmol) was mixed in about 100 µL DAC cream and applied at the time of the challenge and 12 h post challenge on the ventral and dorsal sides of the ear. Mice were kept under anesthesia for 15 min to ensure absorption.

### Franz-diffusion cell assay

After sacrifice, the ears of the mice were tape stripped 10 times, incubated for 1 min in antibiotic/antimycotic reagent (Thermo Fisher), and separated into dorsal and ventral halves. The dorsal side was put on the lower chamber of an unjacketed Franz-diffusion cell (2 mL volume, 5-mm pore), with the dermal side facing the receptor chamber (PermeGear). DAC cream with or without fluorescently labeled AJ102.29 or AJ102.29ctrl (10 pmol per mg) was applied on the epidermal side of the skin. Donor and receptor chamber were

tightly sealed with a clamp. The receptor chamber was filled with 2 mL RPMI (RPMI + 10% FCS, penicillin-streptomycin, L-glutamine). After a 24-h incubation period on a magnetic stirrer at 37°C 5% $CO_2$ the Franz-diffusion cell was disassembled and the residual cream on the skin removed. The skin was gently tapped with a Hank's balanced salt solution-drained tissue to remove the excess cream. Subsequently, the skin sample was embedded into a cryo freezing medium (Sakura Finetek Tissue-Tek O.C.T. Compound, Fisher Scientific), and 10-µm sections were prepared for staining.

#### Immunofluorescence

The slides were thawed for 10 min at room temperature, washed with DPBS for 5 min, and followed by a DAPI (Vectorlab) (1:10,000 in PBS) staining and a second washing step with DPBS before mounting in Mowiol/DABCO. Microscopy was performed with a BZ-9000 digital microscope (Keyence) using the 20× and 40× magnifications.

#### Statistical analysis

Data were tested for statistical significance with GraphPad Prism 9 (GraphPad Software) using 1-way or 2-way ANOVA with the Bonferroni post hoc test for multiple comparisons. The level of significance was denoted as $*p = 0.01–0.05$, $**p = 0.001–0.01$, $***p < 0.001$, $****p < 0.0001$, as indicated in the figure legends.

## DATA AND CODE AVAILABILITY

The data that support the findings of this study are available from the corresponding authors on request.

## SUPPLEMENTAL INFORMATION

Supplemental information can be found online at https://doi.org/10.1016/j.omtn.2024.102254.

## ACKNOWLEDGMENTS

We are grateful to Philip Hatzfeld for technical help. This work was supported by the Deutsche Forschungsgemeinschaft (DFG, German Research Council) through MA3442/8-1 (to G.M.), FO 178/3-1 (to I.F.), GRK2873 (project no. 494832089) (to G.M.), EXC 2151 (project no. 390873048) (to I.F.), and GRK2168 (project no. 272482170) (to I.F.). All animal experiments were approved by the government of North Rhine-Westphalia (Az. 81-02.04.2021.A092).

## AUTHOR CONTRIBUTIONS

A.J. designed and performed the experiments and wrote the manuscript. M.G. designed and performed the experiments and wrote the manuscript. M.S.J.M. performed the innate immune response experiments. Y.M. and M.W.T. assisted with the mouse breeding and animal experiments. L.-C.B. contributed to the establishment of the *ex vivo* skin assay. H.W. guided the generation of the CCL22$^{-/-}$ mice and helped with critical advice. E.L. supervised the innate immune stimulation experiments. G.M. conceived the study, designed the experiments, obtained the funding, and wrote and edited the manuscript. I.F. conceived the study, designed the experiments, obtained the funding, and wrote and edited the manuscript. All authors read, commented on, and approved the final version of the manuscript.

## DECLARATION OF INTERESTS

The authors declare no competing interests.

## REFERENCES

1. Salah, S., Taieb, C., Demessant, A.L., and Haftek, M. (2021). Prevalence of skin reactions and self-reported allergies in 5 countries with their social impact measured through quality of life impairment. Int. J. Environ. Res. Public Health *18*, 4501. https://doi.org/10.3390/IJERPH18094501.

2. Omrane, A., Khedher, A., Harrathi, C., Maoua, M., Khalfallah, T., Bouzgarrou, L., Mrizak, N., Henchi, M.A., and Ali, H.B.H. (2022). Quality of Life of Healthcare Workers Suffering from Occupational Contact Dermatitis. Recent Adv. Inflamm. Allergy Drug Discov. *15*, 44–51. https://doi.org/10.2174/1872213X14666210303155135.

3. Silverberg, J.I., Gelfand, J.M., Margolis, D.J., Boguniewicz, M., Fonacier, L., Grayson, M.H., Simpson, E.L., Ong, P.Y., and Chiesa Fuxench, Z.C. (2018). Patient burden and quality of life in atopic dermatitis in US adults: A population-based cross-sectional study. Ann. Allergy Asthma Immunol. *121*, 340–347. https://doi.org/10.1016/j.anai.2018.07.006.

4. Diepgen, T.L., Ofenloch, R.F., Bruze, M., Bertuccio, P., Cazzaniga, S., Coenraads, P.J., Elsner, P., Goncalo, M., Svensson, Å., and Naldi, L. (2016). Prevalence of contact allergy in the general population in different European regions. Br. J. Dermatol. *174*, 319–329. https://doi.org/10.1111/BJD.14167.

5. Kaplan, D.H., Igyártó, B.Z., and Gaspari, A.A. (2012). Early immune events in the induction of allergic contact dermatitis. Nat. Rev. Immunol. *12*, 114–124. https://doi.org/10.1038/nri3150.

6. Landsteiner, K., and Jacobs, J. (1936). Studies on the sensitization of animals with simple chemical compounds. J. Exp. Med. *64*, 717–722. https://doi.org/10.1084/jem.64.5.717.

7. Vocanson, M., Hennino, A., Chavagnac, C., Saint-Mezard, P., Dubois, B., Kaiserlian, D., and Nicolas, J.-F. (2005). Contribution of CD4+ and CD8+ T-cells in contact hypersensitivity and allergic contact dermatitis. Expert Rev. Clin. Immunol. *1*, 75–86. https://doi.org/10.1586/1744666x.1.1.75.

8. Sebastiani, S., Albanesi, C., De Pità, O., Puddu, P., Cavani, A., and Girolomoni, G. (2002). The role of chemokines in allergic contact dermatitis. Arch. Dermatol. Res. *293*, 552–559. https://doi.org/10.1007/S00403-001-0276-9.

9. Yoshie, O., and Matsushima, K. (2015). CCR4 and its ligands: From bench to bedside. Int. Immunol. *27*, 11–20. https://doi.org/10.1093/intimm/dxu079.

10. Matsuo, K., Nagakubo, D., Komori, Y., Fujisato, S., Takeda, N., Kitamatsu, M., Nishiwaki, K., Quan, Y.S., Kamiyama, F., Oiso, N., et al. (2018). CCR4 Is Critically Involved in Skin Allergic Inflammation of BALB/c Mice. J. Invest. Dermatol. *138*, 1764–1773. https://doi.org/10.1016/j.jid.2018.02.027.

11. Viney, J.M., Andrew, D.P., Phillips, R.M., Meiser, A., Patel, P., Lennartz-Walker, M., Cousins, D.J., Barton, N.P., Hall, D.A., and Pease, J.E. (2014). Distinct Conformations of the Chemokine Receptor CCR4 with Implications for Its Targeting in Allergy. J. Immunol. *192*, 3419–3427. https://doi.org/10.4049/jimmunol.1300232.

12. Ying, S., O'Connor, B., Ratoff, J., Meng, Q., Fang, C., Cousins, D., Zhang, G., Gu, S., Gao, Z., Shamji, B., et al. (2008). Expression and Cellular Provenance of Thymic Stromal Lymphopoietin and Chemokines in Patients with Severe Asthma and Chronic Obstructive Pulmonary Disease. J. Immunol. *181*, 2790–2798. https://doi.org/10.4049/jimmunol.181.4.2790.

13. Luu Quoc, Q., Moon, J.Y., Lee, D.H., Ban, G.Y., Kim, S.H., and Park, H.S. (2022). Role of Thymus and Activation-Regulated Chemokine in Allergic Asthma. J. Asthma Allergy *15*, 157–167. https://doi.org/10.2147/JAA.S351720.

14. Nakatani, T., Kaburagi, Y., Shimada, Y., Inaoki, M., Takehara, K., Mukaida, N., and Sato, S. (2001). CCR4 memory CD4+ T lymphocytes are increased in peripheral blood and lesional skin from patients with atopic dermatitis. J. Allergy Clin. Immunol. *107*, 353–358. https://doi.org/10.1067/mai.2001.112601.

15. Kusumoto, M., Xu, B., Shi, M., Matsuyama, T., Aoyama, K., and Takeuchi, T. (2007). Expression of chemokine receptor CCR4 and its ligands (CCL17 and CCL22) in

murine contact hypersensitivity. J. Interferon Cytokine Res. *27*, 901–910. https://doi.org/10.1089/JIR.2006.0064.

16. Stutte, S., Quast, T., Gerbitzki, N., Savinko, T., Novak, N., Reifenberger, J., Homey, B., Kolanus, W., Alenius, H., and Förster, I. (2010). Requirement of CCL17 for CCR7- and CXCR4-dependent migration of cutaneous dendritic cells. Proc. Natl. Acad. Sci. USA *107*, 8736–8741. https://doi.org/10.1073/PNAS.0906126107.

17. Alferink, J., Lieberam, I., Reindl, W., Behrens, A., Weiß, S., Hüser, N., Gerauer, K., Ross, R., Reske-Kunz, A.B., Ahmad-Nejad, P., et al. (2003). Compartmentalized production of CCL17 *in vivo*: Strong inducibility in peripheral dendritic cells contrasts selective absence from the spleen. J. Exp. Med. *197*, 585–599. https://doi.org/10.1084/jem.20021859.

18. Fülle, L., Steiner, N., Funke, M., Gondorf, F., Pfeiffer, F., Siegl, J., Opitz, F.V., Haßel, S.K., Erazo, A.B., Schanz, O., et al. (2018). RNA Aptamers Recognizing Murine CCL17 Inhibit T Cell Chemotaxis and Reduce Contact Hypersensitivity In Vivo. Mol. Ther. *26*, 95–104. https://doi.org/10.1016/j.ymthe.2017.10.005.

19. Shimada, Y., Takehara, K., and Sato, S. (2004). Both Th2 and Th1 chemokines (TARC/CCL17, MDC/CCL22, and Mig/CXCL9) are elevated in sera from patients with atopic dermatitis. J. Dermatol. Sci. *34*, 201–208. https://doi.org/10.1016/j.jdermsci.2004.01.001.

20. Følsgaard, N.V., Chawes, B.L.K., Bønnelykke, K., Jenmalm, M.C., and Bisgaard, H. (2012). Cord blood Th2-related chemokine CCL22 levels associate with elevated total-IgE during preschool age. Clin. Exp. Allergy *42*, 1596–1603. https://doi.org/10.1111/J.1365-2222.2012.04048.X.

21. Halling, A.S., Rinnov, M.R., Ruge, I.F., Gerner, T., Ravn, N.H., Knudgaard, M.H., Trautner, S., Loft, N., Skov, L., Thomsen, S.F., et al. (2023). Skin TARC/CCL17 increase precedes the development of childhood atopic dermatitis. J. Allergy Clin. Immunol. *151*, 1550–1557.e6. https://doi.org/10.1016/j.jaci.2022.11.023.

22. Horikawa, T., Nakayama, T., Hikita, I., Yamada, H., Fujisawa, R., Bito, T., Harada, S., Fukunaga, A., Chantry, D., Gray, P.W., et al. (2002). IFN-γ-inducible expression of thymus and activation-regulated chemokine/CCL17 and macrophage-derived chemokine/CCL22 in epidermal keratinocytes and their roles in atopic dermatitis. Int. Immunol. *14*, 767–773. https://doi.org/10.1093/INTIMM/DXF044.

23. Kakinuma, T., Nakamura, K., Wakugawa, M., Mitsui, H., Tada, Y., Saeki, H., Torii, H., Komine, M., Asahina, A., and Tamaki, K. (2002). Serum macrophage-derived chemokine (MDC) levels are closely related with the disease activity of atopic dermatitis. Clin. Exp. Immunol. *127*, 270–273. https://doi.org/10.1046/J.1365-2249.2002.01727.X.

24. Wang, X., Fujita, M., Prado, R., Tousson, A., Hsu, H.C., Schottelius, A., Kelly, D.R., Yang, P.A., Wu, Q., Chen, J., et al. (2010). Visualizing CD4 T-cell migration into inflamed skin and its inhibition by CCR4/CCR10 blockades using *in vivo* imaging model. Br. J. Dermatol. *162*, 487–496. https://doi.org/10.1111/J.1365-2133.2009.09552.X.

25. Lehtimäki, S., Tillander, S., Puustinen, A., Matikainen, S., Nyman, T., Fyhrquist, N., Savinko, T., Majuri, M.L., Wolff, H., Alenius, H., and Lauerma, A. (2010). Absence of CCR4 Exacerbates Skin Inflammation in an Oxazolone-Induced Contact Hypersensitivity Model. J. Invest. Dermatol. *130*, 2743–2751. https://doi.org/10.1038/JID.2010.208.

26. Mirshahpanah, P., Li, Y.Y.Y., Burkhardt, N., Asadullah, K., and Zollner, T.M. (2008). CCR4 and CCR10 ligands play additive roles in mouse contact hypersensitivity. Exp. Dermatol. *17*, 30–34. https://doi.org/10.1111/J.1600-0625.2007.00630.X.

27. Mariani, M., Lang, R., Binda, E., Panina-Bordignon, P., and D'Ambrosio, D. (2004). Dominance of CCL22 over CCL17 in induction of chemokine receptor CCR4 desensitization and internalization on human Th2 cells. Eur. J. Immunol. *34*, 231–240. https://doi.org/10.1002/EJI.200324429.

28. Viney, J.M., Andrew, D.P., Phillips, R.M., Meiser, A., Patel, P., Lennartz-Walker, M., Cousins, D.J., Barton, N.P., Hall, D.A., and Pease, J.E. (2014). Distinct conformations of the chemokine receptor CCR4 with implications for its targeting in allergy. J. Immunol. *192*, 3419–3427. https://doi.org/10.4049/JIMMUNOL.1300232.

29. Eiger, D.S., Boldizsar, N., Honeycutt, C.C., Gardner, J., and Rajagopal, S. (2021). Biased Agonism at Chemokine Receptors. Cell. Signal. *78*, 109862. https://doi.org/10.1016/J.CELLSIG.2020.109862.

30. Curiel, T.J., Coukos, G., Zou, L., Alvarez, X., Cheng, P., Mottram, P., Evdemon-Hogan, M., Conejo-Garcia, J.R., Zhang, L., Burow, M., et al. (2004). Specific recruitment of regulatory T cells in ovarian carcinoma fosters immune privilege and predicts reduced survival. Nat. Med. *10*, 942–949. https://doi.org/10.1038/nm1093.

31. Manresa, M.C. (2021). Animal Models of Contact Dermatitis: 2,4-Dinitrofluorobenzene-Induced Contact Hypersensitivity. Methods Mol. Biol. *2223*, 87–100. https://doi.org/10.1007/978-1-0716-1001-5_7.

32. Shin, H., Prasad, V., Lupancu, T., Malik, S., Achuthan, A., Biondo, M., Kingwell, B.A., Thiem, M., Gottschalk, M., Weighardt, H., et al. (2023). The GM-CSF/CCL17 pathway in obesity-associated osteoarthritic pain and disease in mice. Osteoarthritis Cartilage *31*, 1327–1341. https://doi.org/10.1016/J.JOCA.2023.05.008.

33. Ellington, A.D., and Szostak, J.W. (1990). In vitro selection of RNA molecules that bind specific ligands. Nature *346*, 818–822. https://doi.org/10.1038/346818a0.

34. Tuerk, C., and Gold, L. (1990). Systematic Evolution of Ligands by Exponential Enrichment: RNA Ligands to Bacteriophage T4 DNA Polymerase. Science *249*, 505–510. https://doi.org/10.1126/science.2200121.

35. Lieberam, I., and Förster, I. (1999). The murine beta-chemokine TARC is expressed by subsets of dendritic cells and attracts primed CD4+ T cells. Eur. J. Immunol. *29*, 2684–2694. https://doi.org/10.1002/(SICI)1521-4141(199909)29:09.

36. Zuker, M. (2003). Mfold web server for nucleic acid folding and hybridization prediction. Nucleic Acids Res. *31*, 3406–3415. https://doi.org/10.1093/nar/gkg595.

37. Kikin, O., D'Antonio, L., and Bagga, P.S. (2006). QGRS Mapper: a web-based server for predicting G-quadruplexes in nucleotide sequences. Nucleic Acids Res. *34*, W676–W682. https://doi.org/10.1093/NAR/GKL253.

38. Ni, S., Zhuo, Z., Pan, Y., Yu, Y., Li, F., Liu, J., Wang, L., Wu, X., Li, D., Wan, Y., et al. (2021). Recent Progress in Aptamer Discoveries and Modifications for Therapeutic Applications. ACS Appl. Mater. Interfaces *13*, 9500–9519. https://doi.org/10.1021/ACSAMI.0C05750.

39. Healy, J.M., Lewis, S.D., Kurz, M., Boomer, R.M., Thompson, K.M., Wilson, C., and McCauley, T.G. (2004). Pharmacokinetics and biodistribution of novel aptamer compositions. Pharm. Res. (N. Y.) *21*, 2234–2246. https://doi.org/10.1007/S11095-004-7676-4.

40. Kratschmer, C., and Levy, M. (2017). Effect of Chemical Modifications on Aptamer Stability in Serum. Nucleic Acid Ther. *27*, 335–344. https://doi.org/10.1089/nat.2017.0680.

41. Gloor, M., Hauth, A., and Gehring, W. (2003). O/W Emulsions compromise the stratum corneum barrier and improvedrug penetration. Pharmazie *58*, 709–715.

42. Wen, S., Sun, M., Ye, L., Yang, B., Hu, L., and Man, M.Q. (2021). Topical Applications of a Novel Emollient Inhibit Inflammation in Murine Models of Acute Contact Dermatitis. BioMed Res. Int. *2021*, 5594646. https://doi.org/10.1155/2021/5594646.

43. D'Ambrosio, D., Albanesi, C., Lang, R., Girolomoni, G., Sinigaglia, F., and Laudanna, C. (2002). Quantitative Differences in Chemokine Receptor Engagement Generate Diversity in Integrin-Dependent Lymphocyte Adhesion. J. Immunol. *169*, 2303–2312. https://doi.org/10.4049/JIMMUNOL.169.5.2303.

44. Ajram, L., Begg, M., Slack, R., Cryan, J., Hall, D., Hodgson, S., Ford, A., Barnes, A., Swieboda, D., Mousnier, A., and Solari, R. (2014). Internalization of the chemokine receptor CCR4 can be evoked by orthosteric and allosteric receptor antagonists. Eur. J. Pharmacol. *729*, 75–85. https://doi.org/10.1016/J.EJPHAR.2014.02.007.

45. Yoshie, O. (2021). CCR4 as a Therapeutic Target for Cancer Immunotherapy. Cancers *13*, 5542. https://doi.org/10.3390/CANCERS13215542.

46. Yonekura, K., Kanzaki, T., Gunshin, K., Kawakami, N., Takatsuka, Y., Nakano, N., Tokunaga, M., Kubota, A., Takeuchi, S., Kanekura, T., and Utsunomiya, A. (2014). Effect of anti-CCR4 monoclonal antibody (mogamulizumab) on adult T-cell leukemia-lymphoma: cutaneous adverse reactions may predict the prognosis. J. Dermatol. *41*, 239–244. https://doi.org/10.1111/1346-8138.12419.

47. Duvic, M., Pinter-Brown, L.C., Foss, F.M., Sokol, L., Jorgensen, J.L., Challagundla, P., Dwyer, K.M., Zhang, X., Kurman, M.R., Ballerini, R., et al. (2015). Phase 1/2 study of mogamulizumab, a defucosylated anti-CCR4 antibody, in previously treated patients with cutaneous T-cell lymphoma. Blood *125*, 1883–1889. https://doi.org/10.1182/BLOOD-2014-09-600924.

48. Ogura, M., Ishida, T., Hatake, K., Taniwaki, M., Ando, K., Tobinai, K., Fujimoto, K., Yamamoto, K., Miyamoto, T., Uike, N., et al. (2014). Multicenter phase II study of mogamulizumab (KW-0761), a defucosylated anti-cc chemokine receptor 4 antibody,

in patients with relapsed peripheral T-cell lymphoma and cutaneous T-cell lymphoma. J. Clin. Oncol. *32*, 1157–1163. https://doi.org/10.1200/JCO.2013.52.0924.

49. Suzuki, Y., Saito, M., Ishii, T., Urakawa, I., Matsumoto, A., Masaki, A., Ito, A., Kusumoto, S., Suzuki, S., Hiura, M., et al. (2019). Mogamulizumab Treatment Elicits Autoantibodies Attacking the Skin in Patients with Adult T-Cell Leukemia-Lymphoma. Clin. Cancer Res. *25*, 4388–4399. https://doi.org/10.1158/1078-0432.CCR-18-2575.

50. D'Ambrosio, D., Albanesi, C., Lang, R., Girolomoni, G., Sinigaglia, F., and Laudanna, C. (2002). Quantitative differences in chemokine receptor engagement generate diversity in integrin-dependent lymphocyte adhesion. J. Immunol. *169*, 2303–2312. https://doi.org/10.4049/JIMMUNOL.169.5.2303.

51. Chong, B.F., Murphy, J.-E., Kupper, T.S., and Fuhlbrigge, R.C. (2004). E-selectin, thymus- and activation-regulated chemokine/CCL17, and intercellular adhesion molecule-1 are constitutively coexpressed in dermal microvessels: a foundation for a cutaneous immunosurveillance system. J. Immunol. *172*, 1575–1581. https://doi.org/10.4049/JIMMUNOL.172.3.1575.

52. Katou, F., Ohtani, H., Nakayama, T., Ono, K., Matsushima, K., Saaristo, A., Nagura, H., Yoshie, O., and Motegi, K. (2001). Macrophage-derived chemokine (MDC/CCL22) and CCR4 are involved in the formation of T lymphocyte-dendritic cell clusters in human inflamed skin and secondary lymphoid tissue. Am. J. Pathol. *158*, 1263–1270. https://doi.org/10.1016/S0002-9440(10)64077-1.

53. Reiss, Y., Proudfoot, A.E., Power, C.A., Campbell, J.J., and Butcher, E.C. (2001). CC chemokine receptor (CCR)4 and the CCR10 ligand cutaneous T cell-attracting chemokine (CTACK) in lymphocyte trafficking to inflamed skin. J. Exp. Med. *194*, 1541–1547. https://doi.org/10.1084/JEM.194.10.1541.

54. Zhang, Y., Lai, B.S., and Juhas, M. (2019). Recent Advances in Aptamer Discovery and Applications. Molecules *24*, 941. https://doi.org/10.3390/MOLECULES24050941.

55. Shraim, A.S., Abdel Majeed, B.A., Al-Binni, M.A., and Hunaiti, A. (2022). Therapeutic Potential of Aptamer–Protein Interactions. ACS Pharmacol. Transl. Sci. *5*, 1211–1227. https://doi.org/10.1021/acsptsci.2c00156.

56. Wang, H., Su, Y., Chen, D., Li, Q., Shi, S., Huang, X., Fang, M., and Yang, M. (2023). Advances in the mechanisms and applications of inhibitory oligodeoxynucleotides against immune-mediated inflammatory diseases. Front. Pharmacol. *14*, 1119431. https://doi.org/10.3389/fphar.2023.1119431.

57. Zakrewsky, M., Kumar, S., and Mitragotri, S. (2015). Nucleic acid delivery into skin for the treatment of skin disease: Proofs-of-concept, potential impact, and remaining challenges. J. Control. Release *219*, 445–456. https://doi.org/10.1016/j.jconrel.2015.09.017.

58. Lenn, J.D., Neil, J., Donahue, C., Demock, K., Tibbetts, C.V., Cote-Sierra, J., Smith, S.H., Rubenstein, D., Therrien, J.P., Pendergrast, P.S., et al. (2018). RNA Aptamer Delivery through Intact Human Skin. J. Invest. Dermatol. *138*, 282–290. https://doi.org/10.1016/j.jid.2017.07.851.

59. Shobeiri, S.S., Rezaee, M., Pordel, S., Haghnnavaz, N., Dashti, M., Moghadam, M., and Sankian, M. (2022). Anti-IL-17A ssDNA aptamer ameliorated psoriasis skin lesions in the imiquimod-induced psoriasis mouse model. Int. Immunopharmacol. *110*, 108963. https://doi.org/10.1016/j.intimp.2022.108963.

60. Tolle, F., and Mayer, G. (2016). Preparation of SELEX Samples for Next-Generation Sequencing. Methods Mol. Biol. *1380*, 77–84. https://doi.org/10.1007/978-1-4939-3197-2_6.

61. Opazo, F., Eiden, L., Hansen, L., Rohrbach, F., Wengel, J., Kjems, J., and Mayer, G. (2015). Modular Assembly of Cell-targeting Devices Based on an Uncommon G-quadruplex Aptamer. Mol. Ther. Nucleic Acids *4*, e251. https://doi.org/10.1038/mtna.2015.25.